



ARTEMIS

The Power of Virtual Twins to Fight MASLD

D3.1 – DESCRIPTION OF ALL IMAGE PROCESSING RESEARCH ACTIVITIES

Project Full Title: *AcceleRating the Translation of virtual twins towards a pErsonalised Management of steatotic liver patients*

Project acronym: ARTEMIS

Project type: Horizon Europe | RIA (Topic HORIZON-HLTH-2023-TOOL-05-03)

Grant agreement no: 101136299

Document information:

Deliverable no.	D3.1
Title	Description of all image processing research activities
Work Package	WP3
Dissemination level	PU - Public
Nature	R — Document, report
Responsible partner	ULEI
Main Contact person	Stefan Hoehme
Deliverable due submission date	31/12/2024
Deliverable actual submission date	23/12/2024

Document validation:

Validated by	Name	Organisation short name	Visa
Responsible	Stefan Hoehme, Adrian Friebel	ULEI	OK
Reviewer 1	Julieta Di Marco	MUV	OK
Reviewer 2	Amadeo Ten, Leonor Cerdá, Serena Pisoni, Silvia Navarro	HULAFE	OK

Disclaimer

The opinions stated in this report reflect the opinion of the authors and not the opinion of the European Commission.

All intellectual property rights are owned by the consortium of ARTEMIs under terms stated in their Consortium Agreement and are protected by the applicable laws. Reproduction is not authorised without prior written agreement. The commercial use of any information contained in this document may require a license from the owner of the information.

History of changes:

Change explanation	Pages affected	Change made by (Name & surname)	Date



Table of Contents

INTRODUCTION	4
T3.1 Segmentation & quantification tools.....	4
T3.2 Imaging biomarkers & radiomics.....	6
T3.3 Strategies against scanner heterogeneity.....	9
T3.4 Digital Pathology: automatic quantification parameters.....	10
CONCLUSION	10
FUTURE WORK.....	11
References.....	12

Table of Figures

<i>Figure 1: Segmentation of GS+-Zones and bile canaliculi in brightfield whole slide scan (left) and of bile canaliculi and protrusions in immunofluorescence time series (right).....</i>	<i>4</i>
<i>Figure 2: A) 3D Confocal stack visualizing nuclei (blue), bile canaliculi (green) and sinusoids (yellow). B) 3D tissue reconstruction. C) Bile canaliculi and sinusoid network graphs, used for quantification of network properties.....</i>	<i>5</i>
<i>Figure 3: Akoya multiplex immunofluorescence whole slide scan of human hepatocellular carcinoma resection, with segmentation of nuclei (left). Spatial single cell phenotype map visualizing cell types and states (right).</i>	<i>6</i>
<i>Figure 4: Illustration of different MRI sequences used by ULEI for radiomics analyses.</i>	<i>7</i>
<i>Figure 5: Result of ANTs registration on sagittal and coronal slices of liver MRI. Original and registered images overlapped. Yellow areas show coincidence of image, green and red indicate difference.</i>	<i>8</i>
<i>Figure 6: Sagittal and coronal slice of liver MRI with the TotalSegmentator prediction (green) overlapped. ...</i>	<i>8</i>
<i>Figure 7: Left: Example image of MRI Elastography, Right: Example image of CCTA.....</i>	<i>9</i>



INTRODUCTION

The main objective and scope of this deliverable is the description of harmonization, processing and quantification pipelines in the areas of all medical imaging, including digital pathology (INRIA, **ULEI**, **HULAFE**) focusing to the corresponding data processing and software tools.

T3.1 Segmentation & quantification tools

ULEI has developed customized tools for the segmentation and quantification of large-scale structures (e.g. vessels), as well as tools for identifying precancerous and cancerous regions, enabling the subsequent parameterization of the mechanistic model by establishing and fine-tuning the corresponding segmentation methods. **ULEI** prepared a hybrid-approach integrating Superpixel-based machine learning (ML) and U-Net-based deep-learning to efficiently analyze experimental and clinical data. This approach has integrated into the TiQuant software framework which was also developed at **ULEI**. Due to the diversity of experimental images in terms of modality (2D, 3D, video, brightfield, confocal, two-photon) and specification (e.g., staining, magnification, resolution), along with the simultaneous challenge that also small datasets with few or single images must be suitable for segmentation, **ULEI** has developed and published a ML based tool for interactive segmentation using sparse annotations (Friebel et al. 2022). This supervised ML method learns class membership from superpixels, which are generated through spatially-constrained clustering of pixels with similar color. This process also oversegmented the image into a fixed number of homogeneously colored, contiguous, and compact patches (superpixels, or in 3D supervoxels).

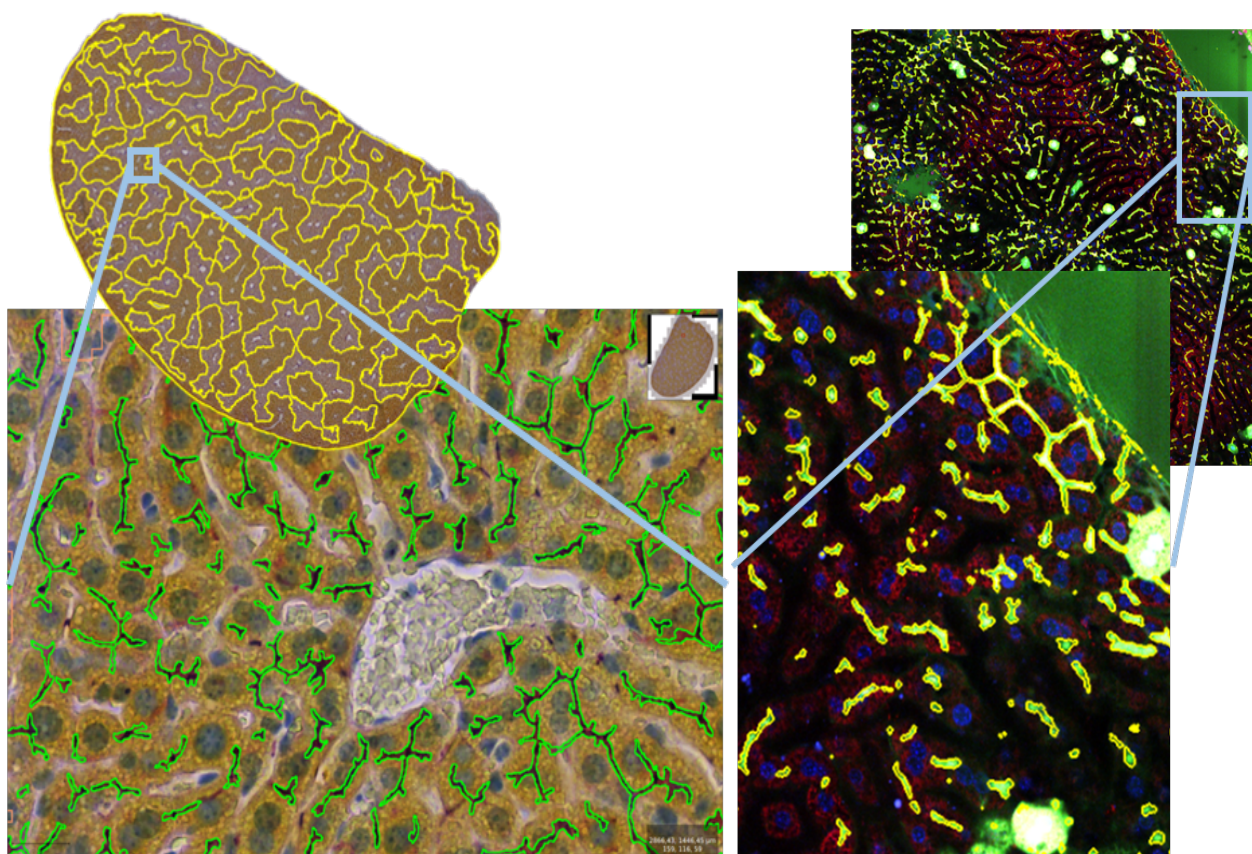


Figure 1: Segmentation of GS+-Zones and bile canaliculi in brightfield whole slide scan (left) and of bile canaliculi and protrusions in immunofluorescence time series (right)

Superpixels can be characterized by color, edge and texture features. The software developed by **ULEI** provides an intuitive graphical user interface that allows the user to annotate sample regions

for the classes to be segmented. A random forest classifier is used to learn superpixel class membership. Trained classifiers can be used to segment visually similar images, however inter-image variability in biomedical datasets is often high, which hampers efficient batch processing. Therefore, **ULEI** developed a two-step k-means based clustering method. In the first step, a set of the most dominant colors is extracted from each image using clustering, while in the second step, the set of dominant colors representing the images in the dataset are clustered to group images with similar coloration. This pre-structuring of the dataset minimizes the number of classifiers to be trained manually for a in-subset reuse. Examples of tissue segmentation are shown in Fig.1. Additionally, the interactive process of image segmentation from sparse annotations is used to provide data for deep-learning-based methods.

Furthermore, **ULEI** established a model zoo for biological and clinical segmentation tasks. This centralized repository contains a collection of pre-trained models, each specifically designed to address a variety of segmentation challenges. These tasks currently encompass the identification of tissue masks in liver and kidney samples and the segmentation of distinct structures (e.g., bile ducts, bile canaliculi) and regions (e.g., areas damaged by cholemic nephropathy) or cells (e.g., endothelial cells) with critical significance in studies related to liver diseases (e.g., cirrhosis, bile duct cancer, hepatitis) or immune system dynamics. The collection of models will be extended for heart tissue upon data availability. The approach of **ULEI** focuses on offering a series of pre-trained models, each defined by detailed specifications of staining protocols and task-specific objectives. These models utilize standardized architectures, such as the nnU-Net v2 framework (Isensee et al. 2020), along with pre-optimized parameters. These models are encapsulated within an out-of-the-box tool designed to ensure consistency and reproducibility across studies and several computational platforms.

ULEI will employ a watershed-based method for reconstructing hepatocytes and liver lobules (Friebel et al. 2015), from segmentations of nuclei, sinusoid and bile canaliculi, or central and portal veins, respectively. This approach complements the liver micro-architecture quantification capabilities previously published (Hammad et al. 2014), which primarily focused on the characterization of the blood vessel and bile canaliculi networks (Fig.2).

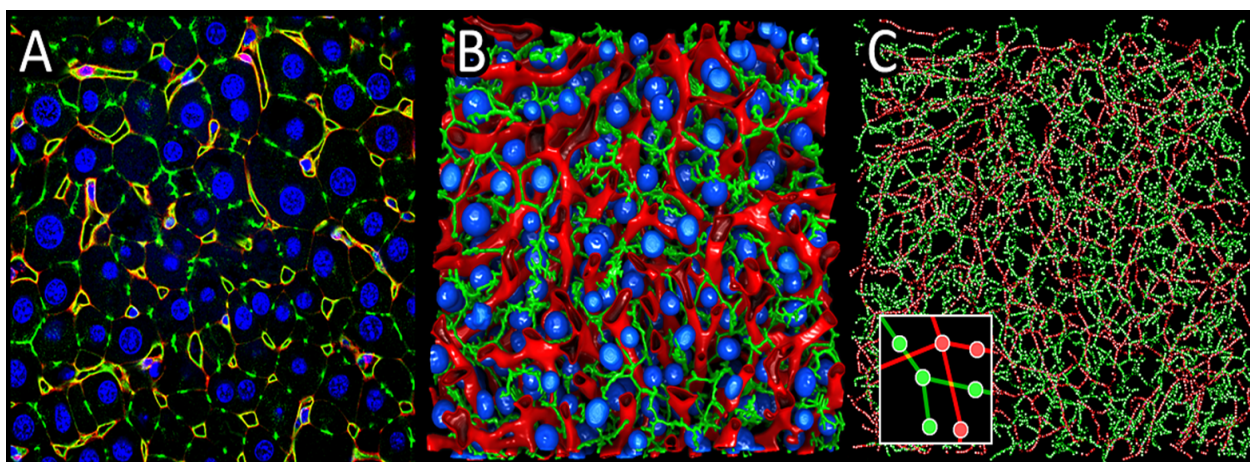


Figure 2: A) 3D Confocal stack visualizing nuclei (blue), bile canaliculi (green) and sinusoids (yellow). B) 3D tissue reconstruction. C) Bile canaliculi and sinusoid network graphs, used for quantification of network properties.

Additionally, **ULEI** has developed a processing tool for the quantification and characterization of tumor microenvironments, such as those derived from multiplex imaging (Fig.3), which is ready for use upon data availability. This tool employs a pretrained Deep Learning (DL) model that enables the segmentation of nuclei and cells using a channel-invariant approach (Goldsborough et al. 2024). Thereby, precise segmentation of nuclei and, especially, cell shapes is achieved, based on markers for various cell types with different morphologies, including hepatocytes, stellate cells and macrophages. **ULEI** is currently developing a prototype workflow for analyzing spatial single-cell data, that allows the quantification of region-specific cell densities and compositions, spatial distances between phenotypes, phenotype interactions and proximities, with potential use in T3.4.

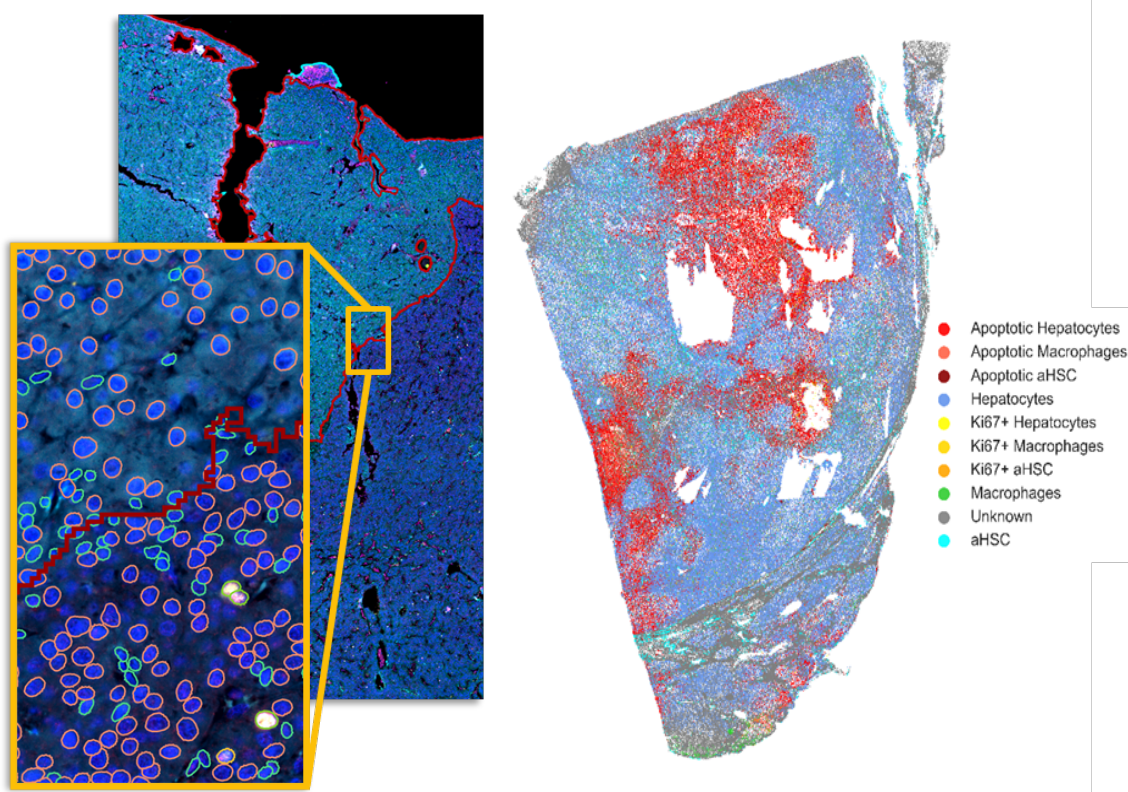


Figure 3: Akoya multiplex immunofluorescence whole slide scan of human hepatocellular carcinoma resection, with segmentation of nuclei (left). Spatial single cell phenotype map visualizing cell types and states (right).

In collaboration with **HULAFE**, **ULEI** coordinated the selection of other existing automatic tools from partners to be used centrally and at each clinical node side on the federated datasets with are now included in the ARTEMIs platform. For example, for the segmentation of Computed Tomography (CT) images, **HULAFE** uses Docker containers based on the open-source tool TotalSegmentator (D'Antonoli et al. 2024), enabling the segmentation of 117 structures, with the liver, heart, and iliopsoas being particularly significant for ARTEMIs. For the segmentation of Magnetic Resonance Imaging (MRI), **HULAFE** has developed a model for automatic liver segmentation from multi-echo sequences (Jimenez-Pastor A et al 2021, Martí-Aguado D et al. 2022) and is currently extending this model to images obtained from mDIXON sequences, especially focusing on the WATER image. Concurrently, **HULAFE** is developing models for the segmentation of spleen, kidney, and fat (visceral and subcutaneous).

The quantification of various imaging biomarkers and deep features extraction at **HULAFE** is not always performed on the same sequences as those used for segmenting the region of interest. Therefore, **HULAFE** uses a tool to register the anatomical sequence/series to which they have a segmentation, with the sequences or series to be quantified, and Elastix® (Klein et al. 2010) to perform these registrations on images in NIFTI format.

T3.2 Imaging biomarkers & radiomics

HULAFE coordinated the selection of imaging biomarkers and quantitative features already developed (Marti-Aguado D et al. 2024, Marti-Aguado D et al. 2022) by the consortium partners, as well as the extraction of radiomics features to be used in ARTEMIs. Furthermore, their relationship with clinical endpoints (sarcopenia, myosteatosi, estimation of ballooning and fibrosis parameters) was discussed within the network. The imaging biomarkers **HULAFE** considers most relevant for ARTEMIs are MRI, Proton Density Fat Fraction (PDFF) (or Fat Fraction (FF) if PDFF is not available, depending on the acquired images) and CT. **HULAFE** has identified three possible methods for obtaining PDFF (Marti-Aguado D et al 2020). 1) If a suitable multi-echo

sequence is available, self-developed Docker containers to obtain PDFF from magnitude images or from magnitude and phase images of each echo, are used as applicable. 2) If InPhase and OutPhase or Water and Fat images, are available, FF can also be calculated. 3) If PDFF or FF maps are directly generated by the MRI scanner, **HULAFE** simply applies the mask to extract the values. Furthermore, for CT, **HULAFE** estimates fat content through Hounsfield Units (HU) thresholding.

Complementary, **ULEI** analyzed exemplary clinical radiology data provided by the University Hospital in Leipzig with regard to morphological and topological measures including radiomics. So far, **ULEI** focused on the integration and analysis of MRI data of the liver, targeting Hepatocellular Carcinoma (HCC) lesions namely abdominal MRI scans, including a series of T1 dynamic contrast-enhanced (DCE) images and various single sequences such as T1 delayed; PDFF images, which quantitatively measures the FF within tissues; Diffusion-Weighted Imaging (DWI) with Apparent Diffusion Coefficient (ADC) maps, which assess the movement of water molecules within tissues and can help identify areas of restricted diffusion, such as in tumors or inflammation; T2-weighted HASTE; T2 Blade Fat-Suppressed (FS); and Magnetic Resonance Elastography (MRE), a non-invasive imaging technique that measures tissue stiffness and is commonly used to evaluate liver fibrosis (Fig.4). The preliminary analyses by **ULEI** included preprocessing, radiomics feature extraction, and classification into risk classes for HCC. To ensure data consistency, preprocessing steps include resampling images to a uniform voxel size, normalization and standardization, and bias field correction to address intensity inhomogeneities.

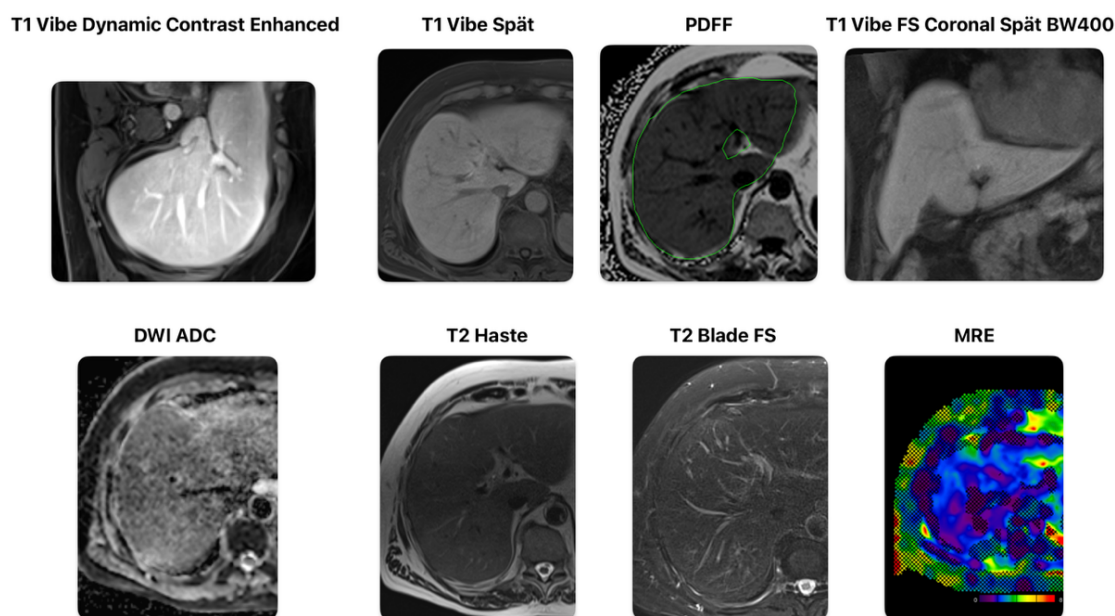


Figure 4: Illustration of different MRI sequences used by **ULEI** for radiomics analyses.

In both CT and MRI, **HULAFE** deployed Docker containers to extract radiomics features (Veiga-Canut D et al. 2024), from the chosen sequence or series. These features can be used for subsequent clustering analysis and pattern recognition (Cerdá Alberich L et al. 2020).

The goal of **MUV** was to model the process from metabolic-associated fatty liver disease (MAFLD) to HCC. The intermediate steps could include prediction of HCC and detection of potentially malignant regions, among others. This will be performed using methods based on ML and DL. Preliminary work of **MUV** is based on a preexisting local cohort. The data in this case contain, ideally, a time series for each involved patient. Currently, **MUV** is working with a local dataset consisting uniquely of MRI scans, and some associated demographic data.

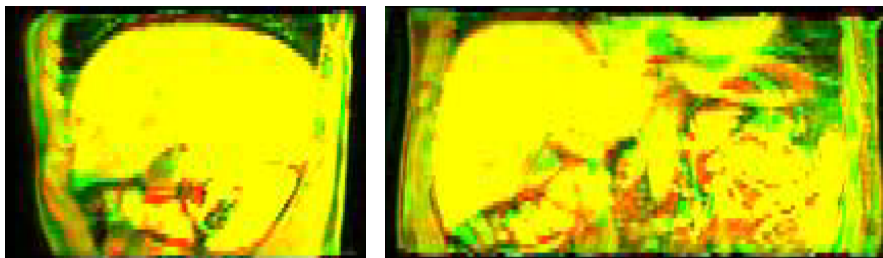


Figure 5: Result of ANTs registration on sagittal and coronal slices of liver MRI. Original and registered images overlapped. Yellow areas show coincidence of image, green and red indicate difference.

Often when working with time series, images need to be registered to consistently identify the same regions of the organ of interest. Registration can be performed intra-patient or inter-patient. The current plan of **MUV** consists of an intra-patient approach. For this VoxelMorph (Balakrishnan et al. 2018) and ANTs (Avants et al. 2009) registration were utilized, with suboptimal results (Fig.5). Upon further observation, **MUV** decided to try using segmentation to support the registration. However, the major morphological and parenchymal variability present in the liver, often due to a progression of the disease under research, make for the registration task to be difficult and arguably incoherent since a lot of the regions become deformed and/or inexistent.

Currently, **MUV** is working on getting a reliable segmentation of the liver. This task has also proven to be quite challenging due to the high heterogeneity of liver morphology; both inter and intra-patient. The current approach relies on 3D-Unet (Wolny et al. 2020) and/or nnU-net (Isensee et al. 2020) architectures. **MUV** is training with annotated (segmented) local images. **MUV** has tried automatic pre-trained tools like TotalSegmentator (D'Antonoli et al. 2024), but the results were suboptimal (Fig.6) and reduced the performance of the registration.

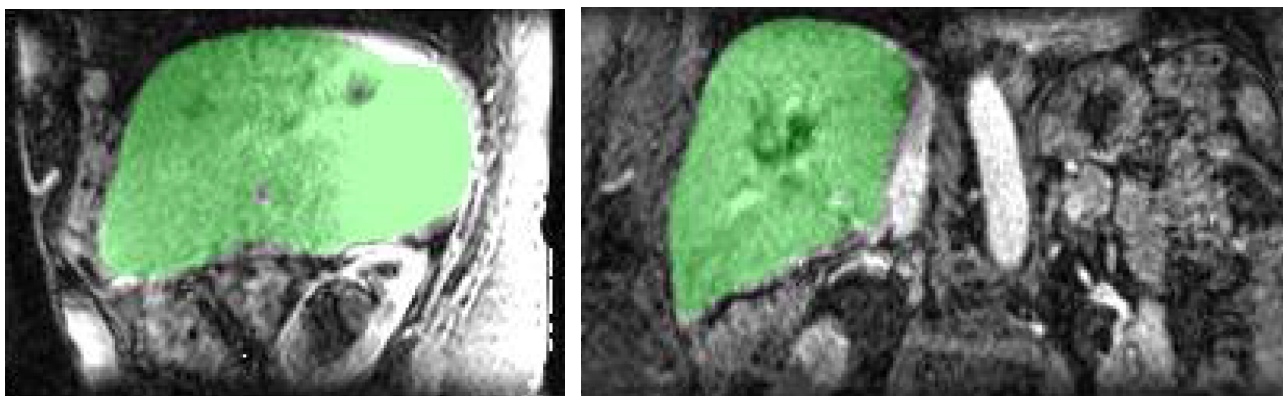


Figure 6: Sagittal and coronal slice of liver MRI with the TotalSegmentator prediction (green) overlapped.

For **MUV**, the goal of the segmentation is to be able to isolate the liver from the image. This would facilitate future models (such as encoders) to learn relevant features that might later be linked to mechanistic models. On the other hand, segmentation of the region of interest is a crucial step for the application of certain ML techniques, such as radiomics (that has shown to provide relevant results in similar problems (Miranda et al. 2023)).

Other processing being carried out by **MUV** is related to the data associated to the images in order to properly curate and describe the cohort. The associated demographic and clinical information could also be used in combination with the imaging data to provide a better prediction on outcomes or analysis of the images.

Quantitative analysis of liver MRI at **ULS** (Fig.7) focuses on measuring stiffness (elastography), hepatic FF, and iron deposition. CT and MRI body composition analysis includes automated segmentation of visceral and subcutaneous fat compartments, muscle mass estimation, and identification of ectopic fat deposition. Quantitative CCTA at **ULS** (Fig.7) includes datasets of

Calcium Scoring (consisting of Agatston score, mass and volume of calcified coronary plaques) and coronary stenosis analysis using dedicated post-processing software.

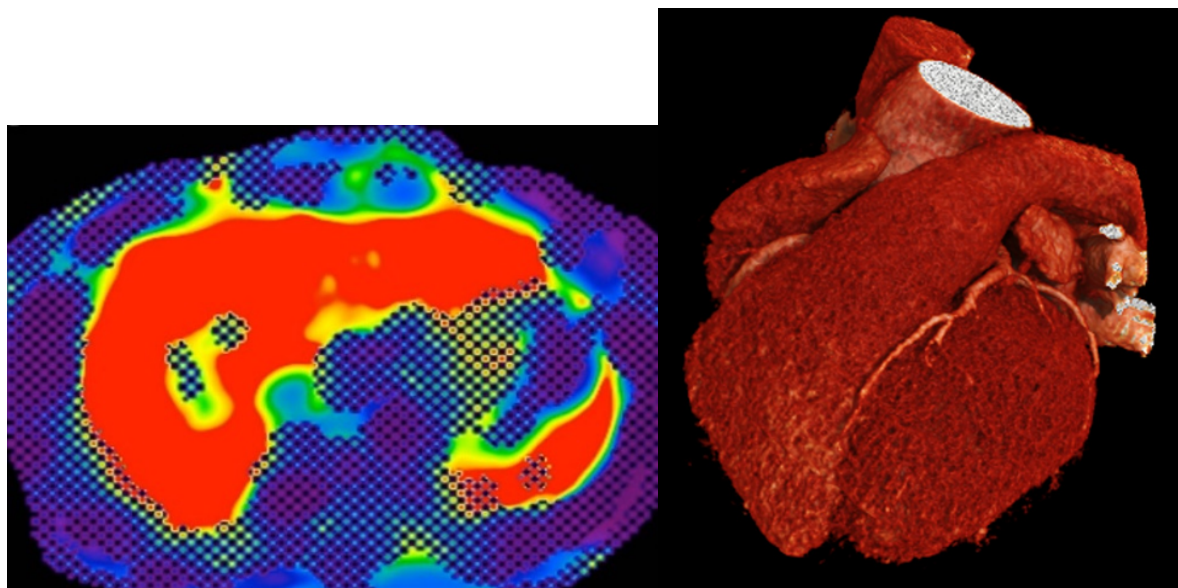


Figure 7: Left: Example image of MRI Elastography, Right: Example image of CCTA

T3.3 Strategies against scanner heterogeneity

MUV is coordinating work on assessing domain adaptation- and continual deep learning approaches for the transfer of image analysis algorithms across sites, or to deal with variability of scanner characteristics. Building upon prior work using rehearsal methods that focus on selecting updated training data (Perkonigg et al. 2021) to maximize the diversity of imaging characteristics in the data. In addition to assessing this method as a means to adapt models across scanners and centers, we are investigating if other characteristics of the disease are reflected in intermediate latent representations of the artificial neural network trained to analyze liver MRI data.

HULAFE implemented several steps to reduce variability introduced by different imaging devices and protocols, ensuring more consistent and comparable datasets for downstream analysis. Initially, a suite of preprocessing techniques was applied by **HULAFE**, including denoising to remove artifacts and reduce the impact of scanner noise on image quality (Fernández Patón M et al 2021, Veiga-Canuto D et al. 2024). Bias field correction addresses intensity inhomogeneities, particularly in MRI, which can arise from uneven magnetic fields or coil sensitivity. Further, all images were spatially rescaled to a common reference size and resolution, enabling uniformity in anatomical representation across datasets. Intensity normalization then adjusts the pixel intensity values to a standard scale, mitigating differences in imaging protocols and enhancing cross-scanner comparability.

Additionally, **HULAFE** proposed implementing advanced harmonization techniques, such as domain adaptation algorithms, which leverage DL or statistical approaches to map data from different scanners into a unified feature space while retaining biologically meaningful information. This can include methods like CycleGANs (Zhu et al. 2017) for scanner-to-scanner image harmonization or ComBat harmonization (Leithner et al. 2023), which corrects for batch effects in imaging data while preserving individual variability. Moreover, quality control measures using both automated tools and expert validation can ensure preprocessing effectiveness and identify residual inconsistencies. These combined strategies can significantly reduce inter-scanner

heterogeneity, enabling more robust and generalizable downstream analyses, such as segmentation or predictive modeling.

In the case of **ULEI**, the data provided by the University Hospital in Leipzig are all sourced from the same scanner type and follow a strict protocol, ensuring consistent parameter settings, except for variations in size and spacing, which can be easily resolved through interpolation. Nevertheless, intra-scanner heterogeneity is addressed through normalization, standardization, and bias field correction. As future analyses may incorporate additional data sources, further preprocessing steps will be applied as needed.

T3.4 Digital Pathology: Automatic quantification parameters

ULEI prepared and fully analyzed several exemplary resected liver tissue samples and biopsies that were stained with antibodies Hoechst (nuclei), Glutamin Synthetase (pericentral parenchyma), Fibronectin (Sinusoids) and Bodipy (Lipid Droplets), imaged using confocal microscopy and subsequently reconstructed, segmented and quantified. The established processing and quantification pipelines for liver tissue (Hammad et al. 2014) that allowed quantification of architectural and dynamic liver parameters (vessel branching properties, diameters of sinusoids and bile canaliculi, density of cells) were complemented by DL based models for the segmentation and subsequent analysis of histology images. The model zoo currently encompasses models for segmentation of necrotic regions from H&E stained images, pericentral zonation markers (GS, OAT, Cyp2e1), periportal zonation markers (CPS1, Arginase-1), nuclei (from H&E or HDAB staining), proliferation (Ki-67), lipid droplets (absent staining), collagen (Sirius Red), immune cells (CD45), bile canaliculi (CD13), bile ducts (CD-19), and endothelial cells (NTCP). **ULEI** used the established software framework TiQuant (Friebel et al. 2015).

HULAFE extracted different biomarkers for each pathological substrate normalized to a reference sample (Marti Aguado D et al. 2020, Marti Aguado D et al. 2021) namely CD45 (percentage of stained areas, number of cell clusters), PERLS (percentage of stained areas (differentiating between diffuse iron and iron granules) and biomarkers derived from the size of the granules), Sirius Red (percentage of stained areas) and Adipophilin (percentage of stained areas (differentiating between microsteatosis and vacuoles) and biomarkers derived from vacuole size).

CONCLUSION

In summary, a multitude of different image analysis approaches and software tools have been prepared and are available to preliminary test data for both histo-pathological microscopic and clinical MRI and CT data. In the process, a collection of suitable biomarkers and software tools has been identified and is now ready to utilize for the patient data collected during the following phases of ARTEMIs. The reduction of unavoidable systemic differences in data due to different on-site technologies (e.g. different microscopes or MRI-machines) are reduced by specific techniques against scanner heterogeneity that will consequently be improved and adapted based on the actual project data. Overall, the preparations of data analysis planned in this deliverable have been successfully achieved.

The main yet unlikely remaining risk that we see is that the actual patient data in ARTEMIs differs significantly from the preliminary test data which would require more effort in adapting our methodology for image analysis that originally was planned.



FUTURE WORK

MUV will continue to work on getting a reliable segmentation for the liver in MRI. Regarding the registration, a different approach is being evaluated where the segmentation of blood vessels would facilitate a consistent segmentation across different time points. Further tasks include the processing of imaging data and associated tabular data, in order to develop models that would be able to predict different aspects of the progression of the disease (such as fibrosis, cirrhosis, malignancies, etc). Eventually, the goal would be to be able to link demographic, clinical and imagenological information as input for a more accurate prediction on disease development. The models would be tested on cohorts from different sites participating of ARTEMIs, providing a more robust and reliable model due to the diversity in patients.

ULEI will expand the model zoo for histology imaging of liver biopsies as needed (e.g., activated stellate cells, cell death marker, ballooned hepatocytes, activated Kupffer cells and hepatic crown-like structures) to complement the established segmentation and quantification methods. This will allow a detailed characterization of disease progression and the tumor micro-environment which will serve as input for the tissue modelling partners. Furthermore, we plan to develop a DL model for the marker-less, staining-invariant segmentation of central and portal veins, arteries and bile ducts, that is robust against the architectural reorganization occurring during disease progression. This model will be linked to a downstream model for the robust reconstruction of liver lobules. In order to achieve a standardized cross-center evaluation of disease progression (e.g., ballooning, fibrosis patterns) that can be related to radiomics features, we will furthermore develop an end-to-end DL model, for histopathological grading.

Future analyses of **ULEI** will integrate radiomics features from additional imaging sequences, supported by robust image registration techniques, to further refine the predictive model. In the long term, we aim to leverage longitudinal imaging data to pinpoint high-risk regions for HCC progression, ultimately improving risk assessment and clinical decision-making.

Once all the MRI studies have been collected, **HULAFE** will propose the final harmonization pipeline for the different imaging modalities (CT, MRI) and set the biomarkers to be extracted from each dataset and each organ.

For the segmentation of the different organs in the different datasets, **HULAFE** will collaborate with **ULEI** to evaluate the performance of each model on each dataset and select or readjust the existing segmentation models to obtain the optimal one in each case.

For digital pathology analysis, **HULAFE** will be able to provide quantification of CD45, PERLS, Sirius Red and Adipophilin staining in patients for which the following stains are available.



References

Avants, Brian; Tustison, Nicholas J.; Song, Gang (2009): Advanced Normalization Tools: V1.0. In: The Insight Journal. DOI: 10.54294/uvnhin.

Balakrishnan, Guha; Zhao, Amy; Sabuncu, Mert R.; Guttag, John; Dalca, Adrian V. (2018): VoxelMorph: A Learning Framework for Deformable Medical Image Registration. DOI: 10.48550/arXiv.1809.05231.

Cerdá Alberich L, Sangüesa Nebot C, Alberich-Bayarri A, Carot Sierra JM, Martínez de Las Heras B, Veiga Canuto D, Cañete A, Martí-Bonmatí L. A Confidence Habitats Methodology in MR Quantitative Diffusion for the Classification of Neuroblastic Tumors. *Cancers (Basel)*. 2020 Dec 21;12(12):3858. doi: 10.3390/cancers12123858. PMID: 33371218; PMCID: PMC7767170.

D'Antonoli, Tugba Akinci; Berger, Lucas K.; Indrakanti, Ashraya K.; Vishwanathan, Nathan; Weiß, Jakob; Jung, Matthias et al. (2024): TotalSegmentator MRI: Sequence-Independent Segmentation of 59 Anatomical Structures in MR images.

Fernández Patón M, Cerdá Alberich L, Sangüesa Nebot C, Martínez de Las Heras B, Veiga Canuto D, Cañete Nieto A, Martí-Bonmatí L. MR Denoising Increases Radiomic Biomarker Precision and Reproducibility in Oncologic Imaging. *J Digit Imaging*. 2021 Oct;34(5):1134-1145. doi: 10.1007/s10278-021-00512-8. Epub 2021 Sep 10. PMID: 34505958; PMCID: PMC8554919.

Friebel, Adrian; Johann, Tim; Drasdo, Dirk; Hoehme, Stefan (2022): Guided interactive image segmentation using machine learning and color-based image set clustering. In: *Bioinformatics (Oxford, England)* 38 (19), S. 4622–4628. DOI: 10.1093/bioinformatics/btac547.

Friebel, Adrian; Neitsch, Johannes; Johann, Tim; Hammad, Seddik; Hengstler, Jan G.; Drasdo, Dirk; Hoehme, Stefan (2015): TiQuant: software for tissue analysis, quantification and surface reconstruction. In: *Bioinformatics (Oxford, England)* 31 (19), S. 3234–3236. DOI: 10.1093/bioinformatics/btv346.

Goldsborough, Thibaut; Philips, Ben; O'Callaghan, Alan; Inglis, Fiona; Leplat, Leo; Filby, Andrew et al. (2024): InstanSeg: an embedding-based instance segmentation algorithm optimized for accurate, efficient and portable cell segmentation.

Hammad, Seddik; Hoehme, Stefan; Friebel, Adrian; Recklinghausen, Iris von; Othman, Amnah; Begher-Tibbe, Brigitte et al. (2014): Protocols for staining of bile canalicular and sinusoidal networks of human, mouse and pig livers, three-dimensional reconstruction and quantification of tissue microarchitecture by image processing and analysis.

Isensee, Fabian; Jaeger, Paul F.; Kohl, Simon A. A.; Petersen, Jens; Maier-Hein, Klaus H. (2020): nnU-Net: a self-configuring method for deep learning-based biomedical image segmentation. In: *Nature Methods*, S. 1–9. DOI: 10.1038/s41592-020-01008-z.

Jimenez-Pastor A, Alberich-Bayarri A, Lopez-Gonzalez R, Marti-Aguado D, França M, Bachmann RSM, Mazzucco J, Marti-Bonmati L. Precise whole liver automatic segmentation and quantification of PDFF and R2* on MR images. *Eur Radiol*. 2021 Oct;31(10):7876-7887. doi: 10.1007/s00330-021-07838-5. Epub 2021 Mar 25. PMID: 33768292.



Klein, Stefan; Staring, Marius; Murphy, Keelin; Viergever, Max A.; Pluim, Josien P. W. (2010): elastix: a toolbox for intensity-based medical image registration. In: IEEE transactions on medical imaging 29 (1), S. 196–205. DOI: 10.1109/TMI.2009.2035616.

Leithner, Doris; Nevin, Rachel B.; Gibbs, Peter; Weber, Michael; Otazo, Ricardo; Vargas, H. Alberto; Mayerhoefer, Marius E. (2023): ComBat Harmonization for MRI Radiomics: Impact on Nonbinary Tissue Classification by Machine Learning. In: Investigative radiology 58 (9), S. 697–701. DOI: 10.1097/RLI.0000000000000970.

Marti-Aguado D, Arnouk J, Liang JX, Lara-Romero C, Behari J, Furlan A, Jimenez-Pastor A, Ten-Esteve A, Alfaro-Cervello C, Bauza M, Gallen-Peris A, Gimeno-Torres M, Merino-Murgui V, Perez-Girbes A, Benlloch S, Pérez-Rojas J, Puglia V, Ferrández-Izquierdo A, Aguilera V, Giesteira B, França M, Monton C, Escudero-García D, Alberich-Bayarri Á, Serra MA, Bataller R, Romero-Gomez M, Marti-Bonmati L. Development and validation of an image biomarker to identify metabolic dysfunction associated steatohepatitis: MR-MASH score. *Liver Int.* 2024 Jan;44(1):202-213. doi: 10.1111/liv.15766. Epub 2023 Oct 30. Erratum in: *Liver Int.* 2024 Nov 26. doi: 10.1111/liv.16190. PMID: 37904633.

Martí-Aguado D, Jiménez-Pastor A, Alberich-Bayarri Á, Rodríguez-Ortega A, Alfaro-Cervello C, Mestre-Alagarda C, Bauza M, Gallén-Peris A, Valero-Pérez E, Ballester MP, Gimeno-Torres M, Pérez-Girbés A, Benlloch S, Pérez-Rojas J, Puglia V, Ferrández A, Aguilera V, Escudero-García D, Serra MA, Martí-Bonmatí L. Automated Whole-Liver MRI Segmentation to Assess Steatosis and Iron Quantification in Chronic Liver Disease. *Radiology.* 2022 Feb;302(2):345-354. doi: 10.1148/radiol.2021211027. Epub 2021 Nov 16. PMID: 34783592.

Marti-Aguado D, Fernández-Patón M, Alfaro-Cervello C, Mestre-Alagarda C, Bauza M, Gallen-Peris A, Merino V, Benlloch S, Pérez-Rojas J, Ferrández A, Puglia V, Gimeno-Torres M, Aguilera V, Monton C, Escudero-García D, Alberich-Bayarri Á, Serra MA, Marti-Bonmati L. Digital Pathology Enables Automated and Quantitative Assessment of Inflammatory Activity in Patients with Chronic Liver Disease. *Biomolecules.* 2021 Dec 2;11(12):1808. doi: 10.3390/biom11121808. PMID: 34944452; PMCID: PMC8699191.

Marti-Aguado D, Rodríguez-Ortega A, Mestre-Alagarda C, Bauza M, Valero-Pérez E, Alfaro-Cervello C, Benlloch S, Pérez-Rojas J, Ferrández A, Alemany-Monrajal P, Escudero-García D, Monton C, Aguilera V, Alberich-Bayarri Á, Serra MÁ, Marti-Bonmati L. Digital pathology: accurate technique for quantitative assessment of histological features in metabolic-associated fatty liver disease. *Aliment Pharmacol Ther.* 2021 Jan;53(1):160-171. doi: 10.1111/apt.16100. Epub 2020 Sep 27. PMID: 32981113

Marti-Aguado D, Rodríguez-Ortega A, Alberich-Bayarri A, Marti-Bonmati L. Magnetic Resonance imaging analysis of liver fibrosis and inflammation: overwhelming gray zones restrict clinical use. *Abdom Radiol (NY).* 2020 Nov;45(11):3557-3568. doi: 10.1007/s00261-020-02713-1. Epub 2020 Aug 28. PMID: 32857259

Martí-Aguado D, Alberich-Bayarri Á, Martín-Rodríguez JL, França M, García-Castro F, González-Cantero J, González-Cantero Á, Martí-Bonmatí L. Differences in multi-echo chemical shift encoded MRI proton density fat fraction estimation based on multifrequency fat peaks selection in non-alcoholic fatty liver disease patients. *Clin Radiol.* 2020 Nov;75(11):880.e5-880.e12. doi: 10.1016/j.crad.2020.07.031. Epub 2020 Sep 2. PMID: 32888653.

Miranda, Joao; Horvat, Natally; Fonseca, Gilton Marques; Araujo-Filho, Jose de Arimateia Batista; Fernandes, Maria Clara; Charbel, Charlotte et al. (2023): Current status and future perspectives of



radiomics in hepatocellular carcinoma. In: *World Journal of Gastroenterology* 29 (1), S. 43–60. DOI: 10.3748/wjg.v29.i1.43.

Perkonigg, M., Hofmanninger, J., Herold, C. J., Brink, J. A., Pinykh, O., Prosch, H., & Langs, G. (2021). Dynamic memory to alleviate catastrophic forgetting in continual learning with medical imaging. *Nature communications*, 12(1), 5678. <https://doi.org/10.1038/s41467-021-25858-z>

Veiga-Canuto D, Fernández-Patón M, Cerdà Alberich L, Jiménez Pastor A, Gomis Maya A, Carot Sierra JM, Sangüesa Nebot C, Martínez de Las Heras B, Pötschger U, Taschner-Mandl S, Neri E, Cañete A, Ladenstein R, Hero B, Alberich-Bayarri Á, Martí-Bonmatí L. Reproducibility Analysis of Radiomic Features on T2-weighted MR Images after Processing and Segmentation Alterations in Neuroblastoma Tumors. *Radiol Artif Intell.* 2024 Jul;6(4):e230208. doi: 10.1148/ryai.230208. PMID: 38864742; PMCID: PMC11294951.

Wolny, Adrian; Cerrone, Lorenzo; Vijayan, Athul; Tofanelli, Rachele; Barro, Amaya Vilches; Louveaux, Marion et al. (2020): Accurate and versatile 3D segmentation of plant tissues at cellular resolution. In: *eLife* 9. DOI: 10.7554/eLife.57613.

Zhu, Jun-Yan; Park, Taesung; Isola, Phillip; Efros, Alexei A. (2017): Unpaired Image-to-Image Translation using Cycle-Consistent Adversarial Networks.

